Frontiers of Physics
https://doi.org/10.1007/s11467-019-0888-1
Front. Phys.
14(3), 31602 (2019)

RESEARCH ARTICLE

Single-step multipartite entangled states generation from coupled circuit cavities

Xiao-Tao Mo, Zheng-Yuan Xue†

Guangdong Provincial Key Laboratory of Quantum Engineering and Quantum Materials, and School of Physics and Telecommunication Engineering, South China Normal University, Guangzhou 510006, China
Corresponding author. E-mail: †*zyxue@scnu.edu.cn*
Received December 19, 2018; accepted February 21, 2019

Green–Horne–Zeilinger states are a typical type of multipartite entangled states, which plays a central role in quantum information processing. For the generation of multipartite entangled states, the single-step method is more preferable as the needed time will not increase with the increasing of the qubit number. However, this scenario has a strict requirement that all two-qubit interaction strengths should be the same, or the generated state will be of low quality. Here, we propose a scheme for generating multipartite entangled states of superconducting qubits, from a coupled circuit cavities scenario, where we rigorously achieve the requirement via adding an extra z-direction ac classical field for each qubit, leading the individual qubit-cavity coupling strength to be tunable in a wide range, and thus can be tuned to the same value. Meanwhile, in order to obtain our wanted multi-qubits interaction, x-direction ac classical field for each qubit is also introduced. By selecting the appropriate parameters, we numerically shown that high-fidelity multi-qubit GHZ states can be generated. In addition, we also show that the coupled cavities scenario is better than a single cavity case. Therefore, our proposal represents a promising alternative for multipartite entangled states generation.

Keywords quantum information processing, quantum entanglement, quantum state engineering

1 Introduction

Entanglement is one of the most counterintuitive consequences of quantum physics, and nowadays it plays a central role in quantum computation and quantum communication [1]. Multipartite entangled states are entangled states of many qubits which are indispensable resource for research in large scale quantum computation [2], multipartite quantum communication [3], quantum simulation [4] and quantum-to-classical transition [5]. Therefore, generating entangled states of an increasing number of qubits is an important benchmark for modern quantum technology [6].

Green–Horne–Zeilinger (GHZ) states [7] are a typical type of maximally entangled states, and the generation of which have been paid much attention recently [8–21]. Conventional way of GHZ states is generated in a step by step way, based on high-fidelity quantum gates. In this way, the number of entangled qubits is only increased by one at a time, and thus the needed generation time will increase with the increasing of the number of the involved qubits. In addition, this method will also result in accumulation of individual gate operation errors when the number of entangled qubits increases. Alternatively, GHZ state can be generated in a single step [22–35], via the deliberately designed collective interaction, irrespective of the number of entangled qubits.

Meanwhile, superconducting transmon qubits, a kind of superconducting Josephson-junction qubit, are one of the promising solid-state processor for quantum state manipulation [36–38]. Recently, the setup of multipartite superconducting qubits connecting to a common bus resonator has been used for single-step entangled state generation. But, with the increasing of the number of qubits, the probability to generate a GHZ state decrease dramatically. This is because that the single-step method has a strict requirement that all the two-qubit interaction strengths should be the same. However, for each qubit, its coupling strength with the bus resonator is different so that the qubit–qubit interaction does not evolve synchronously.

Here, we present a scheme to solve the above-mentioned difficulty in a two coupled cavities scenario, where each superconducting qubit is biased by a z-direction magnetic flux in order to tune the qubit-resonator coupling. Specifically, this modulation can effectively make the qubit-resonator couplings to be tunable via the amplitudes of the external driving fields, so that the same coupling strength requirement for many qubits can be met. Meanwhile, in order to obtain our wanted multi-qubits interaction, different from that of in Refs. [22, 23, 33, 34], x-direction ac classical field for each qubit is also introduced. By se-

*arXiv: 1903.11471.

lecting the appropriate parameters, we analytically proved that multi-qubit GHZ states can be generated and we also numerically simulated the obtained high fidelity. In addition, for the target GHZ generation task, we also numerically show that the coupled cavities scenario is better than a single cavity case. Therefore, our proposal represents a promising alternative for multipartite entangled GHZ states generation with superconducting qubits.

2 The theoretical scheme

The proposed setup for Generating GHZ state is illustrated in Fig. 1, which consists of a two coupled cavity in the circuit QED [37] scenario. Setting $\hbar = 1$ hereafter, the Hamiltonian of the two coupled cavities is

$$\begin{aligned} H_c &= \omega_r a^+ a + \omega_r b^+ b + J(ab^+ + a^+ b) \\ &= \omega_+ P_+^+ P_+ + \omega_- P_-^+ P_-, \end{aligned} \tag{1}$$

where $a^\dagger$ ($b^\dagger$) and a (b) are the creation and annihilation operators for the cavity A (B), respectively; J is the coupling strength between the two cavity modes. The two localized normal modes of this coupled system are $P_\pm = (a \pm b)/\sqrt{2}$, and the frequencies of them are $\omega_\pm = \omega_r \pm J$, with ω_r being chose to be the same for simplicity. Otherwise, the two modes and their frequency will be slightly modified.

In each cavity, there are N transmon qubits, and the free Hamiltonian of them are

$$H_q = \sum_{j=1}^{2N} \frac{\omega_{q_j}}{2} \sigma_j^z, \tag{2}$$

where the static qubit frequencies are $\omega_{q,j}$. The $2N$ qubits

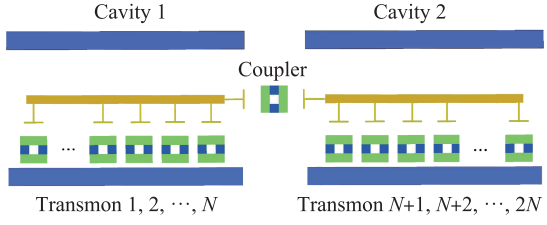

Fig. 1 Schematic diagram of our proposal. The system consists of two cavities coupled by a central coupler, where N transmons qubits (the yellow stripe) are placed in and coupled to each cavity.

are simultaneously coupled to their corresponding cavities, and the coupling Hamiltonian can be generally written as

$$H_{int} = \sum_{j=1}^{N} \frac{g_j}{2} a^+ \sigma_j^- + \sum_{j=N+1}^{2N} \frac{g_j}{2} b^+ \sigma_j^- + H.c., \tag{3}$$

where $\sigma_j^z = |1\rangle_j\langle 1| - |0\rangle_j\langle 0|$, $\sigma_j^+ = |1\rangle_j\langle 0|$, $\sigma_j^- = |0\rangle_j\langle 1|$, with $|0\rangle_j$ and $|1\rangle_j$ being the ground and excited states of jth qubit, g_j is the jth qubit-cavity coupling strength.

Meanwhile, all qubits are simultaneously driven by the classical field along x and z directions as

$$\begin{aligned} H_{dz} &= \sum_{j=1}^{2N} \frac{A_j \sin(\omega_j t + \varphi)}{2} \sigma_j^z, \\ H_{dx} &= \sum_{j=1}^{2N} \frac{\Omega_j}{2} \left(e^{-i\omega_{d_j} t} \sigma_j^+ + e^{i\omega_{d_j} t} \sigma_j^- \right), \end{aligned} \tag{4}$$

where Ω_j is the Rabi frequency of the classical field along x direction and A_j is the amplitude of the classical field which can drive jth qubit along z direction.

In the interaction picture with respect to $H_0 = H_c + H_{dz} + H_q$, the interaction Hamiltonian $H_w = T \exp(i \int H_0 dt)(H_{int} + H_{dx}) T \exp(-i \int H_0 dt)$, with T being the time-ordering operator, will be

$$\begin{aligned} H_w = &\sum_{j=1}^{N} \frac{g_j}{2\sqrt{2}} (P_+^+ e^{i\omega_+ t} + P_-^+ e^{i\omega_- t}) \sigma_j^- e^{-i\omega_{q_j} t} e^{i\alpha_j \cos(\omega_j t + \varphi)} \\ &+ \sum_{j=N+1}^{2N} \frac{g_j}{2\sqrt{2}} (P_+^+ e^{i\omega_+ t} - P_-^+ e^{i\omega_- t}) \sigma_j^- e^{-i\omega_{q_j} t} e^{i\alpha_j \cos(\omega_j t + \varphi)} \\ &+ \sum_{j=1}^{2N} \frac{\Omega_j}{2} e^{-i(\omega_{d_j} t + \varphi_d)} \sigma_j^+ e^{i\omega_{q_j} t} e^{-i\alpha_j \cos(\omega_j t + \varphi)} + H.c. \end{aligned} \tag{5}$$

where $\alpha_j = A_j/\omega_j$. Note that

$$e^{i\alpha_j cos(\omega_j t + \varphi)} \equiv \sum_{m=-\infty}^{\infty} i^m J_m(\alpha_j) e^{im(\omega_j t + \varphi)}, \tag{6}$$

thus setting $\omega_{d_j} = \omega_{q_j}$, $\varphi = \pi/2$, and

$$\begin{aligned} &|\omega_- - \omega_{q_j} + m\omega_j| \gg \{|\delta|, g_j J_1(\alpha_j)\}, \quad m \neq -1 \\ &|\omega_+ - \omega_{q_j} + m\omega_j| \gg \{|\delta|, g_j J_1(\alpha_j)\}, \end{aligned} \tag{7}$$

with $\delta = \omega_- - \omega_{q_j} - \omega_j$, we can neglect the terms oscillating fast, thus Eq. (5) reduces to

$$H'_w = \sum_{j=1}^{2N} \frac{J_0(\alpha_j)\Omega_j}{2} \sigma_j^x + \frac{1}{2\sqrt{2}} \left[\sum_{j=1}^{N} g_j J_1(\alpha_j) e^{i\delta t} P_-^\dagger \sigma_j^- - \sum_{j=N+1}^{2N} g_j J_1(\alpha_j) e^{i\delta t} P_-^\dagger \sigma_j^- + H.c. \right]. \tag{8}$$

Defining $H_{w_0} = \sum_{j=1}^{2N} \frac{J_0(\alpha_j)\Omega_j}{2} \sigma_j^x$. In the interaction picture, the interacting Hamiltonian will be [39]

$$H'_{int} = e^{i\delta t} P_-^\dagger \sum_{j=1}^{N} \frac{g_j}{4\sqrt{2}} J_1(\alpha_j) (\sigma_j^x + |-\rangle_j\langle +| e^{-i J_0(\alpha_j)\Omega_j t} - |+\rangle_j\langle -| e^{i J_0(\alpha_j)\Omega_j t})$$

$$-\mathrm{e}^{\mathrm{i}\delta t}P_{-}^{\dagger}\sum_{j=N+1}^{2N}\frac{g_j}{4\sqrt{2}}J_1(\alpha_j)(\sigma_j^x+|-\rangle_j\langle+|\mathrm{e}^{-\mathrm{i}J_0(\alpha_j)\Omega_j t}-|+\rangle_j\langle-|\mathrm{e}^{\mathrm{i}J_0(\alpha_j)\Omega_j t})+H.c. \tag{9}$$

Assuming that $J_0(\alpha_j)\Omega_j \gg \{\delta, J_1(\alpha_j)g_j\}$, and eliminate the oscillate with high frequencies, H'_{int} reduces to

$$H_{int}=\frac{\mathrm{e}^{\mathrm{i}\delta t}}{4\sqrt{2}}\left[\sum_{j=1}^{N}g_jJ_1(\alpha_j)P_{-}^{\dagger}\sigma_j^x-\sum_{j=N+1}^{2N}g_jJ_1(\alpha_j)P_{-}^{\dagger}\sigma_j^x\right]+H.c.. \tag{10}$$

Note that, in the case, we can control the effective coupling strength g_j by varying the externally the classical field, i.e., by controlling the amplitude α_j, so that

$$g_jJ(\alpha_j)/\sqrt{2}=g \tag{11}$$

can be met. Then H_{int} can be written in the form of

$$H_{int}=\frac{g}{2}P_{-}^{\dagger}J_x\mathrm{e}^{\mathrm{i}\delta t}+H.c., \tag{12}$$

where we have set $J_x=J_1^x-J_2^x$ with $J_1^x=\frac{1}{2}\sum_{j=1}^{N}\sigma_j^x$ and $J_2^x=\frac{1}{2}\sum_{j=N+1}^{2N}\sigma_j^x$.

The evolution operator of the effective Hamiltonian reads

$$U(\gamma)=\exp\left(\mathrm{i}\gamma J_x^2\right)\exp\left(\mathrm{i}BP_{-}^{\dagger}J_x\right)\exp\left(\mathrm{i}B^*P_{-}J_x\right), \tag{13}$$

where

$$\gamma=\frac{g^2}{4\delta}\left[t+\frac{1}{\mathrm{i}\delta}\left(\mathrm{e}^{-\mathrm{i}\delta t}-1\right)\right],$$
$$B=\frac{g}{2\mathrm{i}\delta}\left(\mathrm{e}^{\mathrm{i}\delta t}-1\right). \tag{14}$$

It is obvious that $B(t)$ is a periodic function of time and vanishes at $\delta\tau=2k\pi$ where $k=1,2,3,\cdots$. At those time intervals, the evolution operator in Eq. (13) reduces to

$$U(\tau)=\exp\left[\mathrm{i}\gamma(\tau)J_x^2\right], \tag{15}$$

which can be directly used to generate GHZ states when $\gamma(\tau)=\pi/2$. In this case, $\delta=\sqrt{k}g,\quad \tau=2\pi\sqrt{k}/g$. For a fast scheme, we can set $k=1$.

For an initial state $|\Psi(0)\rangle=|00\cdots0\rangle_a\bigotimes|00\cdots0\rangle_b$ for $2N$ qubits in two cavities a and b, the final state is found to be a GHZ state of

$$|\Psi(\tau)\rangle_N=U\left(\frac{\pi}{2}\right)|\Psi(0)\rangle$$
$$=\frac{1}{\sqrt{2}}\left[|00\cdots0\rangle_a|00\cdots0\rangle_b-\mathrm{i}|11\cdots1\rangle_a|11\cdots1\rangle_b\right], \tag{16}$$

when N is even; the detail derivation are presented in Appendix A.

3 Numerical simulations

In order to obtain the effective Hamiltonian, several approximations have been made here According to the postulated conditions in Eq. (7), we need to choose a suitable value of the frequency ω_j of z-direction magnetic. ω_j is set to around a fixed value, which should be adjusted with respect to the corresponding qubit frequency ω_{qj}, in order to ensure δ to be equal for different qubits. For simplicity, we set $\omega_j/(2\pi)=2\pi\times600$ MHz in our numerical simulation. Meanwhile, suitable driving amplitudes A_js of the z-direction classical fields can be chosen to make sure that the effective qubit-cavity coupling strengths to be the same, as shown in Eq. (11), in spite of the fact that the original qubit-cavity coupling strength g_js are not identical. Here, A_js are used to tune g_j to a same value $g/(2\pi)=15$ (10) MHz in the two (four) qubits case. In addition, since α_j becomes a certain value, we also choose the amplitudes of each x-direction magnetic flux Ω_j to meet the condition of $J_0(\alpha_j)\Omega_j=\Omega$. For our simulation, the used master equation is

$$\frac{\mathrm{d}\rho(t)}{\mathrm{d}t}=-\mathrm{i}\left[H_w,\rho(t)\right]+\kappa L(a)+\kappa L(b)$$
$$+\sum_{j=1}^{2N}\left[\beta L\left(\sigma_j^-\right)+\gamma L\left(\sigma_j^z\right)\right], \tag{17}$$

where $L(B)=B\rho(t)B^{\dagger}-B^{\dagger}B\rho(t)/2-\rho(t)B^{\dagger}B/2$ is the Lindblad operator with $B\in\{a,b,\sigma_j^z,\sigma_j^-\}$. Here, the decay and dephasing rates for all the qubits and the decay for both cavities are all set to be equal as $\kappa=\beta=\gamma=2\pi\times4$ kHz.

As shown in Fig. 2, the fidelities of two qubits entangled state generation are plotted with respective to time, for

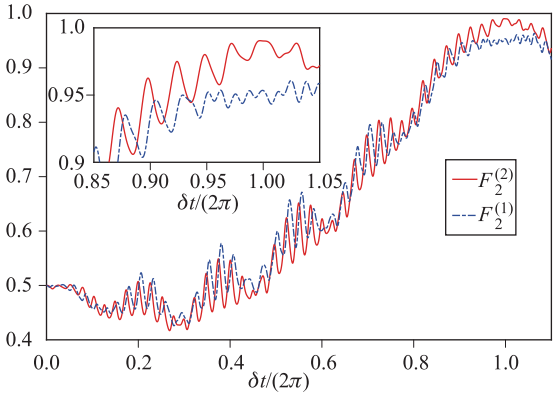

Fig. 2 Time dependence of the fidelity of the two qubits entangled state generation for the two coupled cavities (red solid line) and one cavity (blue dashed line) cases.

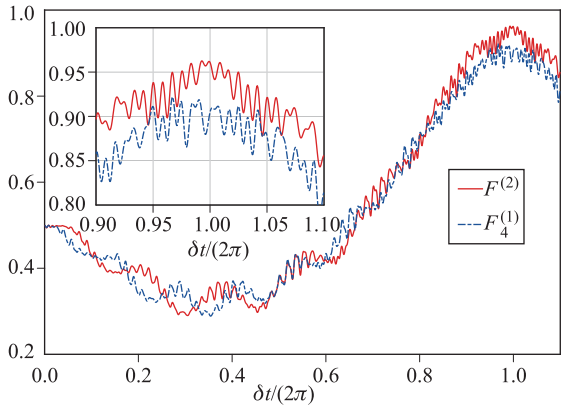

Fig. 3 Time dependence of the fidelity of the four qubits GHZ state generation for the two coupled cavities (red solid line) and one cavity (blue dashed line) cases.

both the one and two cavities cases and the other parameters are list in Table 1. Obviously in Fig. 2, when the $\delta\tau = 2\pi$, the fidelity of red solid line reaches up to 99.02% which is larger than the same data of the blue dashed line. This proves that the performance of generating GHZ state by a z-direction biasing magnetic flux in the two-cavities case is better than that of the one cavity case. Note that, the quantity of inter-cavity coupling J exists only in the two-cavities case, and thus in the one cavity group we compensate this to the qubits' frequency, so that the z-direction driving frequency $\omega_j/(2\pi)$ is still equal to 600 MHz, be consistent with that of the two-cavity case. Besides the number of cavities, decoherence and the oscillating terms are non-negligible factors, which decrease the fidelity of the generated GHZ state. In order to make all qubit-cavity coupling strength g_j to be a same value, each qubit is driven by the classical field along z directions which bring in the oscillating terms that decreases the fidelity about 0.5%. Theoretically, with the increasing of the frequency ω_j, the affect of the oscillating terms would decrease.

Table 1 The chosen parameters for our two qubits entangled state generation schemes.

	Two-cavities case	One-cavity case
α_1	0.5171	0.7025
α_2	0.5036	0.6845
$g_1/(2\pi)$	84.9 MHz	45 MHz
$g_2/(2\pi)$	87.0 MHz	46.5 MHz
$A_1/(2\pi)$	310.26 MHz	421.5 MHz
$A_2/(2\pi)$	302.16 MHz	410.7 MHz
$\Omega_1/(2\pi)$	96.3 MHz	102.2 MHz
$\Omega_2/(2\pi)$	96.0 MHz	101.6 MHz
$\Omega/(2\pi)$	90.0 MHz	90.0 MHz

As shown in Fig. 3, the fidelities of four qubits entangled state generation are plotted with respective to time, for both the one and two cavities cases and the other parameters are list in Table 2. When the $\delta\tau = 2\pi$, the value of fidelity is 96.1% and 90.5% for the two- and one-cavity cases, respectively. The same conclusion we can get is that the two-cavity case shows better performance. Therefore, keeping the qubits apart, e.g., in different cavities, will be beneficial to the increase of fidelity. This is because that the cross talk effect among the oscillating terms will be separated into to cavities and thus some of them have been suppressed.

4 Conclusion

In summary, we have put forward a project to generate GHZ state in two coupled cavities scenario. In this method, each qubit is driven simultaneously by the classical fields. Obviously, the role of the x-direction classical field is manipulating the qubit state. Therefore, we mainly adjust the qubit-cavity strength g_j by controlling the amplitude and frequency of the z-direction classical field. Because of deviation of superconducting manufacturing technique or the other environmental factor, we need a way to make all qubit-cavity coupling strength g_j to be a same value, which can be achieved here by selecting the appropriate parameters. In addition, we also show

Table 2 The chosen parameters for our four qubits entangled state generation shcmes.

	Two-cavities case	One-cavity case
α_1	1.0134	0.7698
α_2	0.9837	0.7389
α_3	0.9562	0.7025
α_4	0.9303	0.6845
$g_1/(2\pi)$	31.8 MHz	28.0 MHz
$g_2/(2\pi)$	32.5 MHz	29.0 MHz
$g_3/(2\pi)$	33.2 MHz	30.0 MHz
$g_4/(2\pi)$	33.9 MHz	31.0 MHz
$A_1/(2\pi)$	608.0 MHz	461.9 MHz
$A_2/(2\pi)$	590.2 MHz	443.3 MHz
$A_3/(2\pi)$	573.7 MHz	421.5 MHz
$A_4/(2\pi)$	558.2 MHz	410.7 MHz
$\Omega_1/(2\pi)$	79.0 MHz	93.3 MHz
$\Omega_2/(2\pi)$	77.7 MHz	92.2 MHz
$\Omega_3/(2\pi)$	76.5 MHz	90.9 MHz
$\Omega_4/(2\pi)$	75.5 MHz	90.3 MHz
$\Omega/(2\pi)$	60.0 MHz	80.0 MHz

that the coupled cavities scenario is better than a single cavity case. Therefore, our proposal represents a promising alternative for multipartite entangled states generation with superconducting qubits.

Acknowledgements This work was supported by the National Natural Science Foundation of China (Grant No. 11874156), the Key R&D Program of Guangdong Province (Grant No. 2018B0303326001), and the National Key R&D Program of China (Grant No. 2016 YFA0301803).

Appendix A Derivation details for Eq. (16)

In this Appendix, we present some derivation details in the maintext. We note that

$$|\Psi(\tau)\rangle_N = \mathrm{e}^{(\mathrm{i}\frac{\pi}{2}J_x^2)}\left|\frac{N}{2},-\frac{N}{2}\right\rangle_{z,a}\left|\frac{N}{2},-\frac{N}{2}\right\rangle_{z,b} = \mathrm{e}^{(\mathrm{i}\frac{\pi}{2}J_x^2)}\sum_{M_1,M_2}C_{M_1}\left|\frac{N}{2},M_1\right\rangle_{x,a}C_{M_2}\left|\frac{N}{2},M_2\right\rangle_{x,b}$$
$$= \sum_{M_1,M_2}\mathrm{e}^{\mathrm{i}\frac{\pi}{2}(M_1-M_2)^2}C_{M_1}\left|\frac{N}{2},M_1\right\rangle_{x,a}C_{M_2}\left|\frac{N}{2},M_2\right\rangle_{x,b}. \tag{A1}$$

As

$$\exp\left[\mathrm{i}\frac{\pi}{2}(M_1-M_2)^2\right] = \begin{cases}\mathrm{i}, & M_1-M_2 \text{ is odd;}\\ 1, & M_1-M_2 \text{ is even.}\end{cases} = \frac{1}{\sqrt{2}}\left[\mathrm{e}^{\mathrm{i}\frac{\pi}{4}}+(-1)^{(M_1-M_2)}\mathrm{e}^{-\mathrm{i}\frac{\pi}{4}}\right]$$
$$= \frac{1}{\sqrt{2}}\left[\mathrm{e}^{\mathrm{i}\frac{\pi}{4}}+(-1)^{2N-2M_1+(M_1-M_2)}\mathrm{e}^{-\mathrm{i}\frac{\pi}{4}}\right]$$
$$= \frac{1}{\sqrt{2}}\left[\mathrm{e}^{\mathrm{i}\frac{\pi}{4}}+(-1)^{N}(-1)^{(N/2-M_1)}(-1)^{(N/2-M_2)}\mathrm{e}^{-\mathrm{i}\frac{\pi}{4}}\right], \tag{A2}$$

we get

$$|\Psi(\tau)\rangle_N = \frac{1}{\sqrt{2}}\sum_{M_1,M_2}\left[\mathrm{e}^{\mathrm{i}\frac{\pi}{4}}+(-1)^{N}(-1)^{(N/2-M_1)}(-1)^{(N/2-M_2)}\mathrm{e}^{-\mathrm{i}\frac{\pi}{4}}\right]C_{M_1}\left|\frac{N}{2},M_1\right\rangle_{x,a}C_{M_2}\left|\frac{N}{2},M_2\right\rangle_{x,b}$$
$$= \frac{1}{\sqrt{2}}\left[\mathrm{e}^{\mathrm{i}\frac{\pi}{4}}\sum_{M_1}C_{M_1}\left|\frac{N}{2},M_1\right\rangle_{x,a}\sum_{M_2}C_{M_2}\left|\frac{N}{2},M_2\right\rangle_{x,b}\right.$$
$$\left.+(-1)^{N}\mathrm{e}^{-\mathrm{i}\frac{\pi}{4}}\left(\sum_{M_1}(-1)^{(N/2-M_1)}C_{M_1}\left|\frac{N}{2},M_1\right\rangle_{x,a}\right)\left(\sum_{M_2}(-1)^{(N/2-M_2)}C_{M_2}\left|\frac{N}{2},M_2\right\rangle_{x,b}\right)\right]$$
$$= \frac{1}{\sqrt{2}}\left[\mathrm{e}^{\mathrm{i}\frac{\pi}{4}}\left|\frac{N}{2},-\frac{N}{2}\right\rangle_{z,a}\left|\frac{N}{2},-\frac{N}{2}\right\rangle_{z,b}+(-1)^{N}\mathrm{e}^{-\mathrm{i}\frac{\pi}{4}}\left|\frac{N}{2},\frac{N}{2}\right\rangle_{z,a}\left|\frac{N}{2},\frac{N}{2}\right\rangle_{z,b}\right],$$
$$= \frac{1}{\sqrt{2}}\left[\mathrm{e}^{\mathrm{i}\frac{\pi}{4}}|00\cdots0\rangle_a|00\cdots0\rangle_b+(-1)^{N}\mathrm{e}^{-\mathrm{i}\frac{\pi}{4}}|11\cdots1\rangle_a|11\cdots1\rangle_b\right]. \tag{A3}$$

When $N=1$, the final state is

$$|\Psi(\tau)\rangle_1 = \frac{1}{\sqrt{2}}\left(|0\rangle_a|0\rangle_b+\mathrm{i}|1\rangle_a|1\rangle_b\right). \tag{A4}$$

In the Schrödinger picture, the above state can be written as

$$\frac{1}{\sqrt{2}}\left[(\mathrm{e}^{-\mathrm{i}\frac{\Omega}{2}t}|+\rangle_a+\mathrm{e}^{\mathrm{i}\frac{\Omega}{2}t}|-\rangle_a)(\mathrm{e}^{-\mathrm{i}\frac{\Omega}{2}t}|+\rangle_b+\mathrm{e}^{\mathrm{i}\frac{\Omega}{2}t}|-\rangle_b)+\mathrm{i}(\mathrm{e}^{-\mathrm{i}\frac{\Omega}{2}t}|+\rangle_a-\mathrm{e}^{\mathrm{i}\frac{\Omega}{2}t}|-\rangle_a)(\mathrm{e}^{-\mathrm{i}\frac{\Omega}{2}t}|+\rangle_b-\mathrm{e}^{\mathrm{i}\frac{\Omega}{2}t}|-\rangle_b)\right] \tag{A5}$$

where $|\pm\rangle_a = \mathrm{e}^{\mathrm{i}\Theta_1}|0\rangle \pm \mathrm{e}^{-\mathrm{i}\Theta_1}|1\rangle$ and $|\pm\rangle_b = \mathrm{e}^{\mathrm{i}\Theta_2}|0\rangle \pm \mathrm{e}^{-\mathrm{i}\Theta_2}|1\rangle$ with $\Theta_n = \omega_{q_n}t/2 - \alpha_n\cos(\omega_n t+\varphi)/2$ and $n\in\{1,2\}$.

References

1. M. A. Nielsen and I. L. Chuang, Quantum Computation and Quantum Information, Cambridge: Cambridge University Press, 2000
2. R. Raussendorf and H. J. Briegel, A one-way quantum computer, *Phys. Rev. Lett.* 86(22), 5188 (2001)
3. M. Hillery, V. Bužek, and A. Berthiaume, Quantum secret sharing, *Phys. Rev. A* 59(3), 1829 (1999)
4. S. Lloyd, Universal quantum simulators, *Science* 273(5278), 1073 (1996)

5. A. J. Leggett, Realism and the physical world, *Rep. Prog. Phys.* 71(2), 022001 (2008)
6. P. Zoller, T. Beth, D. Binosi, R. Blatt, H. Briegel, D. Bruss, T. Calarco, J. I. Cirac, D. Deutsch, J. Eisert, A. Ekert, C. Fabre, N. Gisin, P. Grangiere, M. Grassl, S. Haroche, A. Imamoglu, A. Karlson, J. Kempe, L. Kouwenhoven, S. Kröll, G. Leuchs, M. Lewenstein, D. Loss, N. Lütkenhaus, S. Massar, J. E. Mooij, M. B. Plenio, E. Polzik, S. Popescu, G. Rempe, A. Sergienko, D. Suter, J. Twamley, G. Wendin, R. Werner, A. Winter, J. Wrachtrup, and A. Zeilinger, Quantum information processing and communication, *Eur. Phys. J. D* 36(2), 203 (2005)
7. D. M. Greenberger, M. Horne, A. Shimony, and A. Zeilinger, Bells theorem without inequalities, *Am. J. Phys.* 58(12), 1131 (1990)
8. M. Neeley, R. C. Bialczak, M. Lenander, E. Lucero, M. Mariantoni, A. D. O'Connell, D. Sank, H. Wang, M. Weides, J. Wenner, Y. Yin, T. Yamamoto, A. N. Cleland, and J. M. Martinis, Generation of three-qubit entangled states using superconducting phase qubits, *Nature* 467(7315), 570 (2010)
9. C. P. Yang, Q. P. Su, and F. Nori, Entanglement generation and quantum information transfer between spatially-separated qubits in different cavities, *New J. Phys.* 15(11), 115003 (2013)
10. R. Barends, J. Kelly, A. Megrant, A. Veitia, D. Sank, E. Jeffrey, T. C. White, J. Mutus, A. G. Fowler, B. Campbell, Y. Chen, Z. Chen, B. Chiaro, A. Dunsworth, C. Neill, P. O'Malley, P. Roushan, A. Vainsencher, J. Wenner, A. N. Korotkov, A. N. Cleland, and J. M. Martinis, Superconducting quantum circuits at the surface code threshold for fault tolerance, *Nature* 508(7497), 500 (2014)
11. S. L. Su, X. Q. Shao, H. F. Wang, and S. Zhang, Scheme for entanglement generation in an atom-cavity system via dissipation, *Phys. Rev. A* 90(5), 054302 (2014)
12. S. L. Su, Q. Guo, H. F. Wang, and S. Zhang, Simplified scheme for entanglement preparation with Rydberg pumping via dissipation, *Phys. Rev. A* 92(2), 022328 (2015)
13. H. Paik, A. Mezzacapo, M. Sandberg, D. T. McClure, B. Abdo, A. D. Córcoles, O. Dial, D. F. Bogorin, B. L. T. Plourde, M. Steffen, A. W. Cross, J. M. Gambetta, and J. M. Chow, Experimental demonstration of a resonator-induced phase gate in a multiqubit circuit-QED system, *Phys. Rev. Lett.* 117(25), 250502 (2016)
14. C. P. Yang, Q. P. Su, S. B. Zheng, and F. Nori, Entangling superconducting qubits in a multi-cavity system, *New J. Phys.* 18(1), 013025 (2016)
15. L. Dong, Y. F. Lin, Q. Y. Li, H. K. Dong, X. M. Xiu, and Y. J. Gao, Generation of three-photon polarization-entangled decoherence-free states, *Ann. Phys.* 371, 287 (2016)
16. M. X. Dong, W. Zhang, Z. B. Hou, Y. C. Yu, S. Shi, D. S. Ding, and B. S. Shi, Experimental realization of narrowband four-photon Greenberger–Horne–Zeilinger state in a single cold atomic ensemble, *Opt. Lett.* 42(22), 4691 (2017)
17. X. Q. Shao, D. X. Li, Y. Q. Ji, J. H. Wu, and X. X. Yi, Groundstate blockade of Rydberg atoms and application in entanglement generation, *Phys. Rev. A* 96(1), 012328 (2017)
18. R. Y. Yan, Z. B. Feng, C. L. Zhang, M. Li, X. J. Lu, and Y. Q. Zhou, Fast generations of entangled states between a transmon qubit and microwave photons via shortcuts to adiabaticity, *Laser Phys. Lett.* 15(11), 115205 (2018)
19. C. P. Yang, and Z. F. Zheng, Deterministic generation of Greenberger-Horne-Zeilinger entangled states of cat-state qubits in circuit QED, *Opt. Lett.* 43(20), 5126 (2018)
20. X. L. Wang, L. K. Chen, W. Li, H. L. Huang, C. Liu, C. Chen, Y. H. Luo, Z. E. Su, D. Wu, Z. D. Li, H. Lu, Y. Hu, X. Jiang, C. Z. Peng, L. Li, N. L. Liu, Y. A. Chen, C. Y. Lu, and J. W. Pan, Experimental ten-photon entanglement, *Phys. Rev. Lett.* 117(21), 210502 (2016)
21. Z. Jin, S. L. Su, A. D. Zhu, H. F. Wang, and S. Zhang, Engineering multipartite steady entanglement of distant atoms via dissipation, *Front. Phys.* 13(5), 134209 (2018)
22. K. Mølmer and A. Sørensen, Multiparticle entanglement of hot trapped ions, *Phys. Rev. Lett.* 82(9), 1835 (1999)
23. S. B. Zheng, One-step synthesis of multiatom Greenberger-Horne-Zeilinger states, *Phys. Rev. Lett.* 87(23), 230404 (2001)
24. F. Plastina, R. Fazio, and G. Massimo Palma, Macroscopic entanglement in Josephson nanocircuits, *Phys. Rev. B* 64(11), 113306 (2001)
25. S. B. Zheng, Quantum-information processing and multiatom-entanglement engineering with a thermal cavity, *Phys. Rev. A* 66(6), 060303 (2002)
26. D. I. Tsomoko, S. Ashhab, and F. Nori, Fully connected net-work of superconducting qubits in a cavity, *New J. Phys.* 10(11), 113020 (2008)
27. A. Galiautdinov and J. M. Martinis, Maximally entangling tripartite protocols for Josephson phase qubits, *Phys. Rev. A* 78, 010305(R) (2008)
28. J. Zhang, Y. X. Liu, C. W. Li, T. J. Tarn, and F. Nori, Generating stationary entangled states in superconducting qubits, *Phys. Rev. A* 79(5), 052308 (2009)
29. C. L. Hutchison, J. M. Gambetta, A. Blais, and F. K. Wilhelm, Quantum trajectory equation for multiple qubits in circuit QED: Generating entanglement by measurement, *Can. J. Phys.* 87(3), 225 (2009)
30. Y. D. Wang, S. Chesi, D. Loss, and C. Bruder, One-step multiqubit Greenberger–Horne–Zeilinger state generation in a circuit QED system, *Phys. Rev. B* 81(10), 104524 (2010)
31. S. Aldana, Y. D. Wang, and C. Bruder, Greenberger-Horne-Zeilinger generation protocol for N superconducting transmon qubits capacitively coupled to a quantum bus, *Phys. Rev. B* 84(13), 134519 (2011)
32. T. Monz, P. Schindler, J. T. Barreiro, M. Chwalla, D. Nigg, W. A. Coish, M. Harlander, W. Hansel, M. Hennrich, and R. Blatt, 14-qubit entanglement: Creation and coherence, *Phys. Rev. Lett.* 106(13), 130506 (2011)

33. Y. P. Zhong, D. Xu, P. Wang, C. Song, Q. J. Guo, W. X. Liu, K. Xu, B. X. Xia, C. Y. Lu, S. Han, J. W. Pan, and H. Wang, Emulating anyonic fractional statistical behavior in a superconducting quantum circuit, *Phys. Rev. Lett.* 117(11), 110501 (2016)

34. C. Song, K. Xu, W. Liu, C. Yang, S. B. Zheng, H. Deng, Q. Xie, K. Huang, Q. Guo, L. Zhang, P. Zhang, D. Xu, D. Zheng, X. Zhu, H. Wang, Y. A. Chen, C. Y. Lu, S. Han, and J. W. Pan, 10-qubit entanglement and parallel logic operations with a superconducting circuit, *Phys. Rev. Lett.* 119(18), 180511 (2017)

35. Y. J. Fan, Z. F. Zheng, Y. Zhang, D. M. Lu, and C. P. Yang, One-step implementation of a multi-target-qubit controlled phase gate with cat-state qubits in circuit QED, *Front. Phys.* 14(2), 21602 (2019)

36. J. Q. You and F. Nori, Atomic physics and quantum optics using superconducting circuits, *Nature* 474(7353), 589 (2011)

37. M. H. Devoret and R. J. Schoelkopf, Superconducting circuits for quantum information: An outlook, *Science* 339(6124), 1169 (2013)

38. X. Gu, A. F. Kockum, A. Miranowicz, Y. Liu, and F. Nori, Microwave photonics with superconducting quantum circuits, *Phys. Rep.* 718-719, 1 (2017)

39. E. Solano, G. S. Agarwal, and H. Walther, Strong-driving-assisted multipartite entanglement in cavity QED, *Phys. Rev. Lett.* 90(2), 027903 (2003)